



Use of hybrid filters to optimize the process of the filtration in cement particles

Flávia M. Oliveira da Silva^{a,*}, Luiz Guilherme M. da Silva^b, Ana C.A. Justi^c,
Marcos V. Rodrigues^d, Mônica L. Aguiar^c

^a School of Agriculture, Polytechnic Institute of Beja, Portugal

^b Federal Institute of Education, Science and Technology of the South of Minas- Campus Machado, Brazil

^c Department of Chemical Engineering, Federal University of São Carlos, Brazil

^d Department of Chemical Engineering, Federal University of Alfenas, Brazil

ARTICLE INFO

Keywords:

Electrostatic charger
Dust cake
Cement
Bag filter
Air filtration

ABSTRACT

Due to growing concern about air pollution and its harmful effects on the health of the population, especially in regard to sub-micrometric particles, some studies have reported that applying an electric field to particle suspensions can improve filter performance by enhancing the deposition of particles in the filter medium. This can result in better particulate retention, which is particularly important for industrial processes such as cement production. The objective of this study was to investigate the behavior of cement particles with electrostatic charges during cake formation in fabric filters. The particles (with a d_{50} % of $17 \mu\text{m}$) were generated using a dust feeder at a flow rate of 0.083 kg s^{-1} . The fiberglass filter medium was subjected to filtration tests with constant dust concentrations ($9\text{--}12 \text{ g.m}^{-3}$) and air surface velocities (6 cm.s^{-1} and 10 cm s^{-1}) until the pressure drop reached the maximum value of 400 Pa . The electrostatic precipitator utilized discharge voltages of $0, 4, 10,$ and 12 kV . The particles were initially passed through the electrostatic precipitator to become charged with voltages of $0, 4, 10,$ and 12 kV applied. The results indicated a reduction in pressure drop of up to 55% . The study observed a change in the deposition behavior of particles on the filter medium surface and in the filter cake formation, demonstrating that the electrostatic charge improves air filtration performance, resulting in higher efficiency and cost-effectiveness.

1. Introduction

Particulate matter emissions from industries and vehicles are recognized as one of the most critical primary pollutant sources in major cities worldwide and pose a risk to the population's health [1,2]. Air pollution directly impacts air quality, which depends on pollutant emissions and weather conditions in a given location. Natural disasters such as floods and cyclones, as well as atmospheric stability conditions, may contribute to the dispersion of pollutants or support their continued presence in the lower atmosphere [3,4].

Due to the strong impacts of atmospheric pollution on the environment and human health, new laws and regulations that prohibit or reduce air pollution are emerging and are increasingly stringent. Many research studies show that cement plants are major sources of particulates polluting the environment. According to Aleksei Kholodov et al. [5], the production of cement, cement materials, and

* Corresponding author.

E-mail address: flavia.silva@ipbeja.pt (F.M. Oliveira da Silva).

<https://doi.org/10.1016/j.heliyon.2023.e21808>

Received 21 June 2023; Received in revised form 19 October 2023; Accepted 29 October 2023

Available online 3 November 2023

2405-8440/© 2023 Published by Elsevier Ltd.

This is an open access article under the CC BY-NC-ND license

(<http://creativecommons.org/licenses/by-nc-nd/4.0/>).

asbestos-cement products is associated with the emissions of dust and particulate matter, carbon monoxide (CO), nitrogen oxides (NO_x), sulfur dioxide (SO₂), and volatile organic compounds. The aerosol pollution also includes industrial dumping of overburdened rock formed during the extraction of raw materials. Pollutants are also formed and emitted during the storage, and all the productive processes of the cement.

In addition to complying with new legislation, there is a focus on recovering the maximum amount of cement powder lost during the process, which is the most profitable product. Consequently, new solutions are emerging for removing fine particulates from a stream of gases, including developing new technologies and adapting existing equipment in industrial plants to meet current environmental regulations. However, some industries are not solely focused on complying with emission limits set by authorities when it comes to filtration processes. They also strive to minimize operating costs [1,6]. Another device that should be highlighted is the electrostatic precipitator (ESP), whose operating principle involves the application of high electric potentials (–30 kV) to discharge electrodes, generating large quantities of electrons that charge the particles so that they can be attracted to collectors by electric forces. These systems provide high collection efficiencies for particles larger than 1 μm, with meagre operational costs, compared to fibre filters [7,8]. However, the efficiency of an electrostatic precipitator decreases for particles smaller than 1 μm, with the lowest collection efficiency for particles in size range 200–500 nm [1,9].

New hybrid filtration systems are being developed to improve the cleaning of gas streams. These systems combine two devices with different operating principles, such as an electrostatic precipitator placed in series with a bag filter, known as a hybrid electrostatic filtration system – HEFS [10,11].

The commercial availability of hybrid filtration systems has increased in recent years due to the requirement for more efficient removal of fine particles (smaller than 1 μm).

In the enhanced electrostatic filtration (EEAF) techniques, an electric field was first applied to the suspension of particles, which then entered the fabric filter and changed the deposition of the particles on the fibres. This results in better performance in terms of both increased filter efficiency and reduction of the pressure drop [9,10,12–14]. Previous studies of hybrid filters by Wang et al. (2014) [15] and Tu et al. (2018) [1] demonstrated that fabric filter performance improved when the particles were charged during air filtration.

According to Jaworek et al., 2019 [6], hybrid electrostatic filters differ from hybrid electrostatic precipitators in that the particles are removed only by the bag filter. An electrostatic pre-charger is used exclusively for particle charging, while in hybrid electrostatic precipitators, the coarse particles are removed by the electrostatic precipitator [16].

Numerous studies have investigated the effect of electrostatic charging on filtration efficiency, although most of these studies involved numerical simulations [1,7,17]. Meanwhile, laboratory studies have focused on characterizing electrostatic charge and filtration efficiency [2,9,18].

The objective of this work was to investigate the behavior of cement particles during the formation of the filtration cake, applying the electrostatic discharge in the particles. The increased porosity of the filtration cake increases the useful life of the bag filters.

2. Experimental

2.1. Materials and methods

The particulate matter (cement) was characterized in the Laboratory of Structural Characterization and Environmental Control at the Department of Chemical Engineering, Federal University of UFSCar (Brazil). X-ray analysis was conducted on the material using an applied voltage of –25 kV. The elements present in the sample are as follows: Ca (74.5 %), Si (11.5 %), Mg (4.1 %), Fe (2.6 %), and Nb (7.3 %) (refer to Fig. 1). The sample exhibits an electrical resistivity of 107 Ω m. Density determination was performed using a digital helium pycnometer (AccuPyc 1330, Micromeritics), yielding a value of $3.1 \pm 0.031 \text{ kg m}^{-3}$. The mean volumetric diameter was

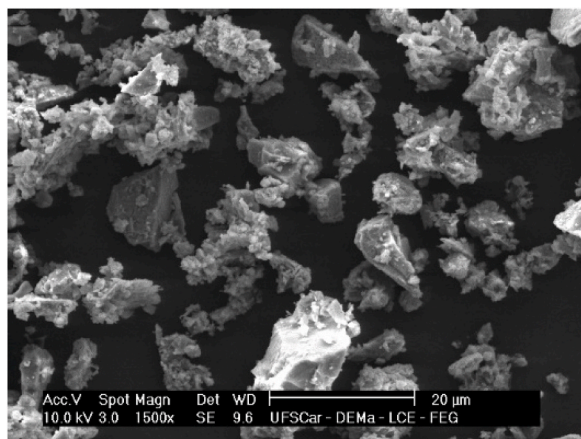
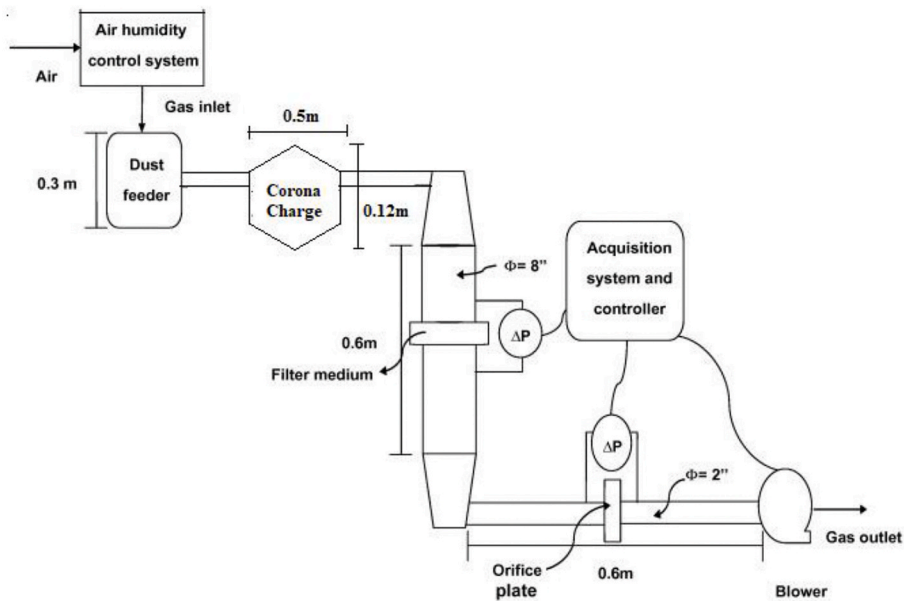


Fig. 1. SEM image of the cement dust.

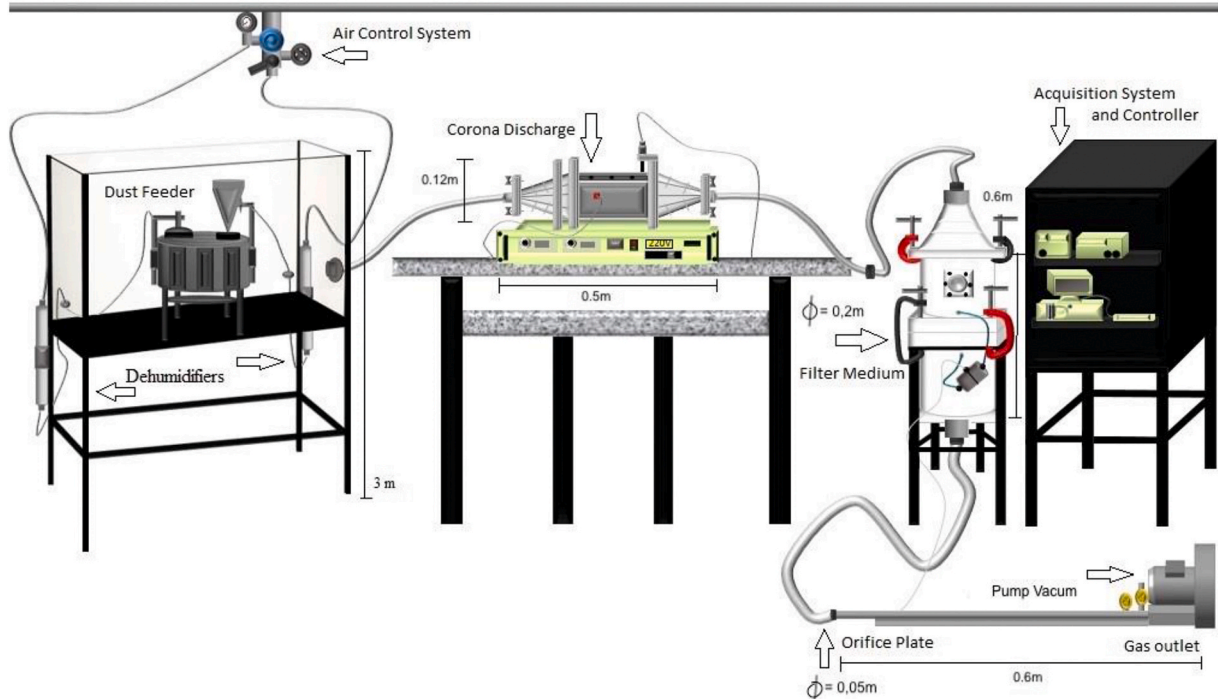
determined utilizing the Mastersizer Microplus 5001 system (Malvern Instruments), resulting in a value of $17.0 \pm 0.13 \mu\text{m}$.

Fig. 1 displays the cement particles as observed under a Carl-Zeiss SEM, model DSM-940-A, at a magnification of $1500\times$. All the particulate material and filters were provide Votorantin Cimentos S.A. Itaú de Minas, Brasil.

The filtration tests employed fiberglass as the filter medium, with a grammage of $750 \text{ g}\cdot\text{m}^{-3}$. This fiberglass filter medium, supplied by BWF in Italy, is a needled felt composed of 100 % polypropylene fiber (3008 PP). The manufacturer, Gino Cacciari, produced it with



a. Experimental equipment



b. Design of Experimental equipment.

Fig. 2. a. Experimental equipment. b. Design of Experimental equipment.

a specific weight of 0.22 g.cm^{-3} and a thickness ranging from 2.5 to 2.8 mm.

The selection of this filter was based on its remarkable efficiency at higher temperatures, a crucial characteristic for cement factories. For the experimental procedures, circular sections of the bag filter, approximately 0.2 m in diameter and weighing about 0.02 kg each, were prepared. These sections boasted a filtration area of 0.0254 m^2 .

The permeability is the porous filter medium property that indicates the ease with which a fluid pass through it [19]. According to Hung and Leung (2011) [20] outlined two distinct approaches for enhancing filter quality. The first entails augmenting its efficacy in aerosol filtration, whereas the second involves enhancing its permeability to mitigate pressure drops [21]. The permeability constant can be derived through the utilization of Forchheimer’s equation. In this equation, the initial term pertains to viscous effects exclusively, while the subsequent term relates to inertial effects, as outlined previously [19].

$$\frac{\Delta P}{L} = \frac{\mu}{K_1} V_s + \frac{\rho}{K_2} r V_s^2 \tag{1}$$

where ΔP is the pressure drop between the inlet and outlet of the filter during passage of the air stream, is a function of the gas flow velocity (V_s) and, consequently, the granular solids, with gradual transition from laminar to turbulent flow [22], L is the thickness of the filter medium, μ is the viscosity of the fluid, k_1 and k_2 are permeability constants of the filter medium, r is the density of the gas, V_s is the superficial velocity. In the present work, a low filtration velocity was used, so the second term of equation (1) could be neglected, becoming the Darcy equation [14,23]:

$$\frac{\Delta P}{L} = \frac{\mu}{K_1} V_s \tag{2}$$

Darcy’s equation, which is used to evaluate the flow of fluids in porous filter media, relating the pressure drop to the superficial velocity. The permeability of the clean filter medium was $2,5.10^{-12} \pm 2,7.10^{-15}$ and the square of the correlation coefficient (R^2) was 0.99.

The procedure adopted for determination of the theoretical cake porosity, using classical equations such as the Ergun equation was based on the method described by Aguiar and Coury (1996) [14,22].

2.2. Experimental equipment

A schematic illustration of the experimental system used in the filtration trials is shown in Fig. 2. The equipment was installed in Environmental Control Laboratory I of the Department of Chemical Engineering at UFSCar.

Fig. 2 shows the layout of the equipment step by step, while Fig. 2b shows the designer with all parts of the equipment in a more illustrative way.

2.3. Experimental procedure

Filtration curves were generated by evaluating the pressure drop across the filter over time, with an anticipated maximum pressure drop of 400 Pa. The particles were introduced into a dish with a velocity of 2 rpm while being conveyed through a stream of dry air via a venturi tube. Prior to deposition onto the filter to form the dust cake, the particles underwent electrostatic charging using a charging device. Gas filtration experiments were conducted under a consistent superficial velocity of 0.05 m/s, and the particle concentration spanned from 9 to 12 g.m^{-3} .

Although the typical filtration velocity for dust collection often hovers around 0.016 m s^{-1} , in this study, a filtration velocity of

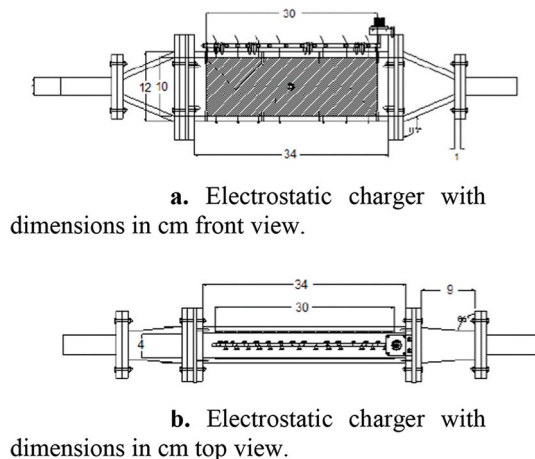


Fig. 3. a. Electrostatic charger with dimensions in cm front view. b. Electrostatic charger with dimensions in cm top view.

$0.05 \text{ m}\cdot\text{s}^{-1}$ was employed. This choice was influenced by certain findings in the literature, such as the work of Donovan et al. (1982) [18]. The experimental protocol adhered to the guidelines outlined in Ref. [14].

After the filtration tests, an analysis of particle deposition was performed according to the same procedure used for experimental porosity determination, developed by Ref. [14]. This procedure conferred good structural stability of the gas filter cake to obtain the images by SEM. For this, the particles deposited in the filter medium were submitted to pre-hardening by passing a flow of adhesive vapor, to fix the particles in the filter fibers. The samples were then hardened, sectioned, embedded, and polished. After these preparation steps, the samples were metalized with gold and scanning electron microscopy images (XL-30 FEG-SEM, Philips), to count the number and determine the depth in the filter and porosity. The images were analyzed using Image-Pro Plus 7.0 software, with binarization to improve the contrast between the pores and the fibers of the sample, hence providing greater reliability in the parameter determination. These techniques have been used by several researchers [24,25] with the same objective.

2.4. Description electrostatic charger

The particulate charger consists of an acrylic box filled with cylindrical stainless-steel wires 5 discharge electrodes were positioned vertically with the same spaces between each other. At the upper end, the electrodes are connected to a high voltage source, brand Spellman, and model S11200, responsible for the application of a potential between 0 and 12 kV. Fig. 3a shows the front view and Fig. 3b the top view of the equipment with all descriptions about size.

3. Results and discussion

3.1. Current-voltage characteristics of corona pre-charger

To determine the precise point of the onset of corona charging (disruption of the dielectric gas), a current-voltage curve was generated at a gas velocity of $0.05 \text{ m}\cdot\text{s}^{-1}$. The ambient humidity was kept at approximately 20 %, and the temperature was monitored and found to have an average value of 26°C throughout the experiment. The average ambient pressure was 0.92 atm. The initial tests were conducted without any particles present in the gas flow ($0 \text{ g}\cdot\text{m}^{-3}$), followed by the introduction of cement particles into the gas stream at a concentration of $11.8 \text{ g}\cdot\text{m}^{-3}$.

In Fig. 4, it can be observed that the electrical current changes as the voltage applied to the airflow increases. The experiment was conducted by passing clean air ($0 \text{ g}\cdot\text{m}^{-3}$) through the electrostatic precipitator at a constant speed, while increasing the voltage of the precipitator in steps of 1 kV. The corona charger started when the voltage reached the value of 10 kV ($5.0 \text{ kV}\cdot\text{cm}^{-1}$), and the dielectric gas rupture occurred at -17.5 kV ($-8.75 \text{ kV}\cdot\text{cm}^{-1}$). However, when the air was loaded with cement particles ($11.8 \text{ g}\cdot\text{m}^{-3}$) and flowed through the precipitator, the same corona current point was obtained at 10 kV ($5.0 \text{ kV}\cdot\text{cm}^{-1}$), but the dielectric gas rupture occurred at -15 kV ($-7.5 \text{ kV}\cdot\text{cm}^{-1}$).

The study involving high voltages requires caution, as voltages above the corona current can lead to the generation of electrical arcs, as shown in Fig. 5. An electric arc was formed in the airflow without particles at an applied voltage of $-8.5 \text{ kV}\cdot\text{cm}^{-1}$ and a current of 1.4 mA. This visual result allowed the experiment to limit the stress values applied for the safety of the operator.

The electrostatic precipitator conditions did not affect the filter medium, and the filtration efficiency was not impacted by the air filter. The tests were performed in triplicate for both cases, and corona current values were measured from an applied voltage of 10 kV.

3.2. Analysis of particle deposition in the corona-effect filter

Filtration time is a significant parameter in the gas filtration process. The longer the filtration time for a cycle, the lower the wear of

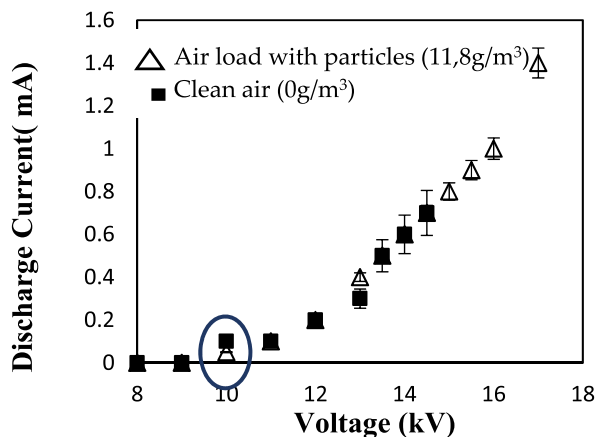


Fig. 4. Relation between voltage and the discharge current.



Fig. 5. The exact moment of generated electrical arcs.

the bags throughout the process. As shown in Fig. 6a, the filtration curves corresponding to the corona effect being active (10 and 12 kV) exhibited the longest filtration duration under a constant superficial velocity of 0.05 m s^{-1} , with particle concentrations ranging from 9 to 12 g.m^{-3} . Due to the use of the electrostatic precipitator, there was a reduction in the number of particles that went to the filter, and this caused the filtration to become longer. For the 10 and 12 kV applied to the particles, increasing them by 100 % and 400 %, respectively, the filtration time compared to the curve of 0 kV was possible. The 4 kV curve did not obtain a relevant difference compared to the 0 kV curve when compared to the others. Fig. 6b shows the behaviour of the particles' pressure drop to deposited mass. For the 4 kV applied can be seen that obtained the highest mass with the lowest time; this occurred because the flow of particulate matter that arrived in the filter was higher due to the electrostatic precipitator functioning only as an electrostatic charger.

The rapid flow of particles during filtration can or not result in a large amount of particles accumulating on the filter medium, leading to the formation of a very compact filtration cake that accelerates the wear of the bags. While filtration time is an important parameter in gas filtration, there are other relevant parameters to consider, such as the mass of particles retained by the filter medium. Fig. 7 shows the graph of the mass of particles retained on the filter medium as a function of time.

Long-term experiments were conducted by Shi and Ekberg (2015) [13] using a hybrid electrostatic filter to investigate filter degradation over 200 days of operation. A synthetic M6-class filter was tested in the laboratory and installed in an office ventilation system, operating with and without preloaded particles. Results showed that filtration efficiency was consistently about 40 % higher when particle preloading was used [2].

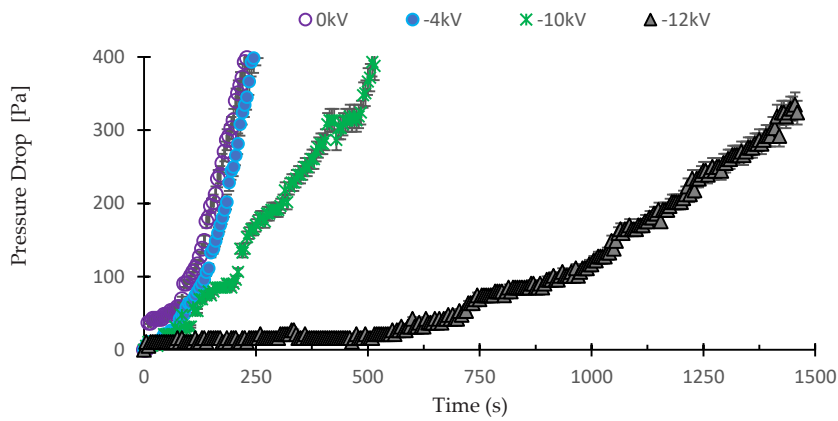
Walsh. (1996) [26] reported that bridging is faster for smaller particles. It is believed that this may be one of the factors involved in this work because for curves with an active corona effect (10 and 12 kV), the electrostatic precipitator acted as a collector where the larger particles were collected, so most of the particulate material that reached the tissue filter presented a smaller granulometry.

Table 1 shows the diameter of the particle on the dust cake surface by the MASTERSIZER MALVERN v.2.19. These results prove the efficiency of the electrostatic precipitator and the change in the behaviour of the particles during the deposition on the filter.

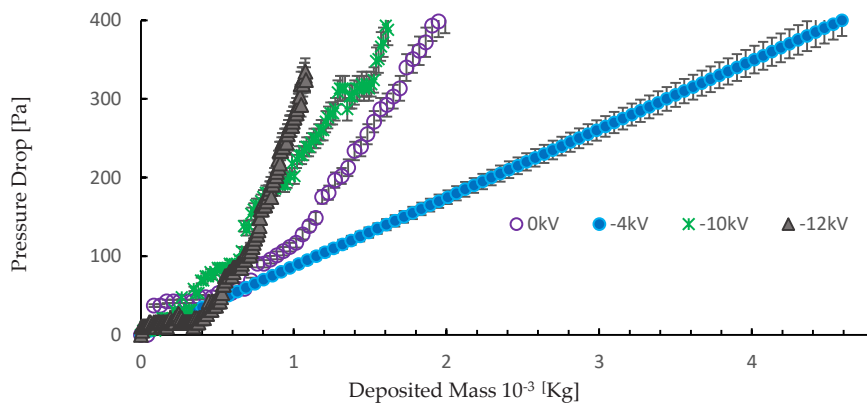
A larger amount of particles on the filter surface was observed for voltages of 0 and 4 kV, as shown in Fig. 8(a; b). However, for voltages of 10 and 12 kV, the amount of particles deposited on the filter medium was lower than the applied load of 4 kV (Fig. 8(c; d)). It was also observed that some filter fibers began to appear in Fig. 8d. This behavior can be attributed to particle loading, as the electrostatic precipitator retained larger particles and just smaller particles arrived on filter, when used 10 and 12 kV, as shown in Table 1.

For the tests of (a) 0 kV and (b) 12 kV images were obtained with a magnification of $800\times$. It was verified that for the filtration cake without electrostatic charge applied, it is possible to observe a greater amount of cement particles with larger diameters deposited on the surface of the fibers, already for the filtration cake with the applied load of 12 kV, particle size appeared to be much smaller compared to 0 kV filtration dust cake. Median diameter of $20.98 \mu\text{m}$ was obtained for 0 kV, and $2.98 \mu\text{m}$ to 12 kV, these values are presented in Table 1. Compare both respectively, the results obtained was for deposited mass 3,17 g to 1,04 g; filtration time 415s–1455s and pressure drop 398Pa–324Pa.

This happened because the feed flow of powder going to filter decreased dramatically from 0 to 12 kV, but if you compare by final



a. Filtration’s curves pressure drop x time.



b. Filtration’s curves pressure drop x deposited mass.

Fig. 6. a. Filtration’s curves pressure drop x time. b. Filtration’s curves pressure drop x deposited mass.

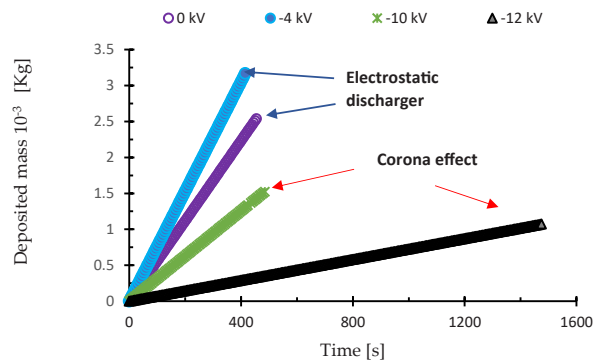


Fig. 7. Filtration’s curves retained mass x time.

pressure drop, the amount of mass collected for 300Pa was higher than for 12 kV. However, due to the lower dust flow of smaller diameters, the filtration time increased and the particle deposition in the fibers was longer, this can lead to the formation of more compact pies and difficulties in removing the pie at the time of cleaning the sleeves.

It can be observed that for the filtration sample without an applied load (0 kV), the particles were deposited both on the fibers and

Table 1
Diameter on dust cake surface (μm) by Malvern.

Tension (kV)	Diameter on dust cake surface (μm) Malvern
0	$20,98 \pm 0,79$
4	$5,50 \pm 14,2$
10	$4,45 \pm 24,6$
12	$2,98 \pm 26,7$

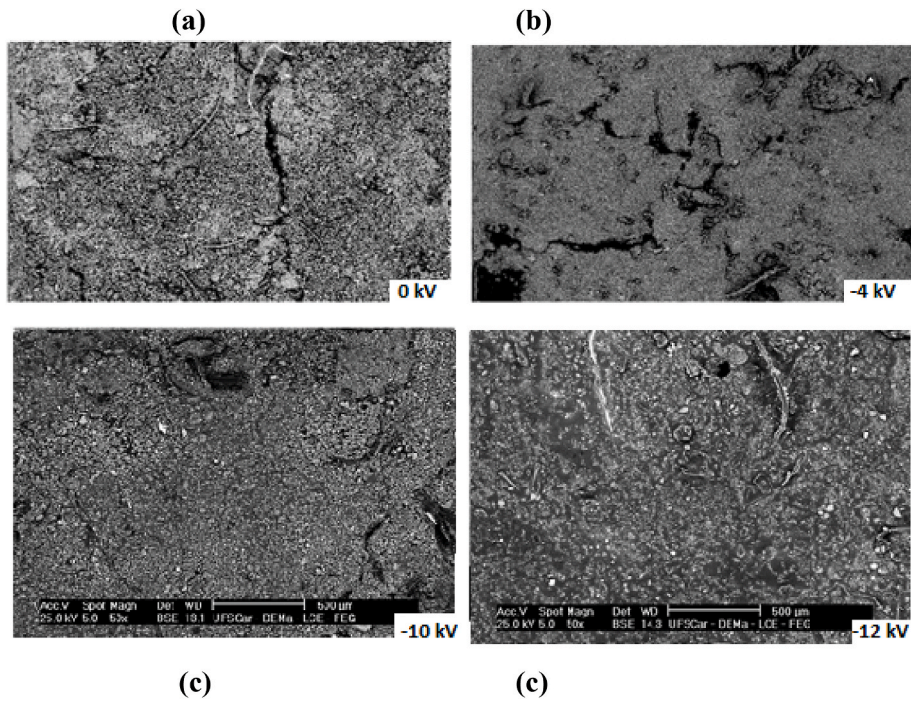


Fig. 8. Images of the filtration dust cake with the inlay of the dust cake, top view obtained through the SEM with magnification of $35\times$, for the applied load of 0 kV (a), 4 kV (b), 10 kV (c) and 12 kV (d).

in the empty spaces between the fibers.

The deposition occurred both between the fiber and particle and between particle-particle, forming dendrites and resulting in a layer of powder between the pores of the filter medium. On the other hand, for the applied load of 12 kV (Fig. 9b), it can be clearly observed that the particles were predominantly deposited on the fibers of the filter medium and formed clusters in the empty spaces between the fibers, with a particle-fiber deposition pattern.

The results suggest in the presence of an electric field, at least part of the particles that came out of the ESP without being collected carried electrical charges. Consequently, in addition to the mechanical mechanisms of particle collection by the fibers of the filter

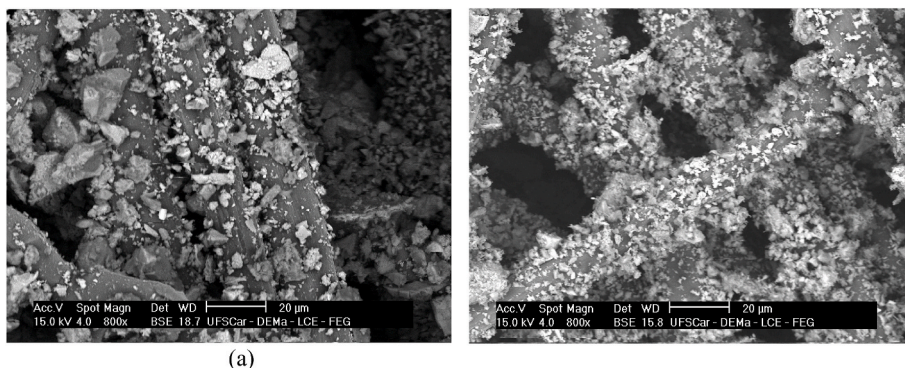


Fig. 9. Images of the inside of the filter through the SEM with magnification of $800\times$, load applied 0 kV (a) and with applied load of 12 kV (b).

medium, there was also the action of the electrostatic mechanism. If the fibers of the filter media did not contain electrical charges, the electrostatic attraction occurred through the action of the image force, generated by the polarization of the fibers due to the presence of electrical charges in the particles [18,27].

Moreover, previous works have shown that the formation of dendrites is favored by the presence of electrical charges in the particles, especially in the early stages of depth filtration. Such formations favor the collection of subsequent particles, as they have the same diameter and project from the fibers into the gas stream [1,28].

Huang et al. (2006) [29], studied the deposition of volatile ash particles on tissue fibers during gas filtration using corona loading and induced polarization. The deposition of particles in the initial filtration was analyzed, and the result showed that the charged particles were deposited in the fibers of the tissue and were forming short and straight chains, with uniform distances. The same behavior can be observed in Fig. 9 (b) for a 12 kV load, the particles are mostly distributed evenly, and it can be noted that the particle size distribution by the fibers is apparently homogeneous.

Some researchers have described the behavior of particle deposition in the filter.

Feng et al. (2016) and Liu et al. (2016) [9,31], highlighted the increase in collection efficiency in the hybrid electrostatic precipitator, where the larger particles were retained, and the fine particles charged by the corona effect were carried by the air flow to the bag filter. The electrical charge of the particles coming out of the electrostatic precipitator facilitated the formation of more porous dendrites in the surface and the bag filter which facilitates their cleaning.

However, there is a disadvantage in the hybrid electrostatic precipitator, when the charged fine particles leave the precipitator, they can form more compact pies in the bag filter than the thick particles. Liu et al. (2016) [30] showed that the concentration of particles greater than 10 μm deposited in the bag filter decreases from 85 % to 20 % (by mass), while the concentration of particles smaller than 2.5 μm increases from 2 to 26 % (by mass), with electrostatic loading on, [6].

On the other hand, one of the advantages of hybrid electrostatic precipitators is the decrease in the penetration of particles into the filter, which can facilitate the cleaning process of the sleeves.

The penetration of particles into a tissue filter decreases with electrostatic loading during filtration and depends on parameters such as particle size distribution, particle concentration, surface gas velocity, and temperature [1,31].

The porosity values of the filtration dust cake increased for the particles loaded with the corona effect (10 and 12 kV), as can be seen in Table 2 the porosity obtained by the Ergun Equation for a load of 10 kV was 0.62 and the experimental porosity was 0.65 the difference in percentage between the two results was approximately 5 %.

For the load of 12 kV obtained porosities of 0.51 and 0.53 by the Ergun equation and by the direct method, respectively, the value of the difference between these results was 4 %. The porosity decreased with the load of 12 kV compared to 10 kV, means formation of a more compacted cake.

The areas of empty spaces were calculated from Fig. 8 and the results are shown in Tables 2 and it was verified that as the electrostatic charge was applied to the particles the area of empty spaces increased. The best result was obtained for a load of 10 kV with a value of 14.9 mm^2 this is related to the highest porosity values between 0.62 and 0.65 and the value of the specific resistance of the pie that decreased to a load of 10 kV obtaining a value of $75.3 \cdot 10^{-3} \text{ s}^{-1}$.

For Xia, S et al. [32], there is a lack of a significant correlation between particle penetration and particle size, regardless of the surface velocity of the gas. It is known that it is possible to reduce the penetration of particles using a higher electrostatic charge in gas filtration, as shown in Fig. 9.

4. Conclusions

The laboratory-developed technique used to capture images from the filters was found to be highly effective to observe changes in particle behavior during the formation of a dust cake inside the filter.

The results demonstrate the superior efficiency of electrostatic particle loading compared to conventional gas filtration. Specifically, the study shows that by using electrostatic loading, larger particles can be effectively retained while allowing smaller particles to reach the filter medium. Furthermore, when these smaller particles are electrostatically charged, they exhibit altered deposition patterns within the filter fibers.

The deposition of cement particles in the filter was improved, which decreased the pressure drop across the filter and increased the porosity of the dust cake. This change in the formation of the dust cake can result in a longer useful life for bag filters, leading to cost savings for companies and reducing environmental impact by reducing the need for frequent filter replacements.

Future studies could be particularly exciting if they investigate the behavior of particles during the formation of a dust cake in other types of fabric filters, using different particulate materials. Such investigations could yield valuable insights into filtration mechanisms and help advance our understanding of this important field.

Data availability

Data availability statement.

Additional information

No additional information is available for this paper.

Table 2

Values of Ergun porosity, experimental porosity, and area of empty spaces.

Tension (kV)	Deposited mass in filter (g)	Ergun's Porosity	Experimental Porosity
0	1,99	0,42	0,41
4	4,59	0,40	0,36
10	1,61	0,62	0,65
12	1,08	0,51	0,53

CRedit authorship contribution statement

Flávia M. O da Silva: Writing – review & editing, Writing – original draft, Visualization, Validation, Methodology, Investigation, Formal analysis, Data curation, Conceptualization. **Luiz G.M. da Silva:** Writing – review & editing, Visualization, Validation. **Ana C.A. Justi:** Writing – review & editing, Visualization, Data curation. **Marcos V. Rodrigues:** Writing – review & editing, Methodology, Conceptualization. **Mônica L. Aguiar:** Writing – review & editing, Supervision, Resources, Methodology, Conceptualization.

Declaration of competing interest

The authors declare that they have no known competing financial interests or personal relationships that could have appeared to influence the work reported in this paper.

Acknowledgements

The authors would like to thank Coordination for the Improvement of Higher Education Personnel (CAPES) for funding the student scholarship.

References

- [1] G. Tu, Q. Song, Q. Yao, Mechanism study of electrostatic precipitation in a compact hybrid particulate collector, *Powder Technol.* 328 (2018) 84–94, <https://doi.org/10.1016/j.powtec.2018.01.016>.
- [2] R. Zhang, J. Jing, J. Tao, S.C. Hsu, G. Wang, J. Cao, Z. Shen, Chemical characterization and source apportionment of PM 2.5 in Beijing: seasonal perspective, *Atmos. Chem. Phys.* 13 (14) (2013) 7053–7074.
- [3] World Health Organization (WHO), Health topics: chronic respiratory diseases?, Available online: https://www.who.int/health-topics/chronic-respiratory-diseases-tab=tab_1. (Accessed 12 February 2023).
- [4] F.M.O. Silva, E.C. Alexandrina, A.C. Pardal, M.T. Carvalhos, E. Schornobay Lui, Monitoring and prediction of particulate matter (PM_{2.5} and PM₁₀) around the ipbeja campus, *Sustainability* 14 (2022), 16892, <https://doi.org/10.3390/su142416892>.
- [5] Aleksei Kholodov, Zakharenko Alexander, Vladimir Drozd, Valery Chernyshev, Konstantin Kirichenko, Ivan Seryodkin, Karabtsov Alexander, Svetlana Olesik, Ekaterina Khvost, Igor Vakhnyuk, Vladimir Chaika, Antonios Stratidakis, Marco Vinceti, Dimosthenis Sarigiannis, A. Wallace Hayes, Aristidis Tsatsakis, Kirill Golokhvast, Identification of cement in atmospheric particulate matter using the hybrid method of laser diffraction analysis and Raman spectroscopy, *Heliyon* 6 (2) (2020), e03299, <https://doi.org/10.1016/j.heliyon.2020.e03299>. ISSN 2405-8440.
- [6] A. Jaworek, A.T. Sobczyk, A. Krupa, A. Marchewicz, T. Czech, L. Śliwiński, Hybrid electrostatic filtration systems for fly ash particles emission control, A review. *Separation and Purification Technology* 213 (2019) 283–302, <https://doi.org/10.1016/j.seppur.2018.12.011>.
- [7] K. Adamiak, Numerical models in simulating wire-plate electrostatic precipitators: a review, *J. Electrostat.* 71 (4) (2013) 673–680, <https://doi.org/10.1016/j.elstat.2013.03.001>.
- [8] H.J. Kim, B. Han, Y.J. Kim, S.J. Yoa, Characteristics of an electrostatic precipitator for submicron particles using non-metallic electrodes and collection plates, *J. Aerosol Sci.* 41 (11) (2010) 987–997, <https://doi.org/10.1016/j.jaerosci.2010.08.001>.
- [9] Z. Feng, W. Pan, H. Zhang, X. Cheng, Z. Long, J. Mo, Evaluation of the performance of an electrostatic enhanced air filter (EEAF) by a numerical method, *Powder Technol.* 327 (2018) 201–214, <https://doi.org/10.1016/j.powtec.2017.12.054>.
- [10] Z. Feng, Z. Long, T. Yu, Filtration characteristics of fibrous filter following an electrostatic precipitator, *J. Electrostat.* 83 (2016) 52–62, <https://doi.org/10.1016/j.elstat.2016.07.009>.
- [11] G. Tu, Q. Song, Q. Yao, Relationship between particle charge and electrostatic enhancement of filter performance, *Powder Technol.* 301 (2016) 665–673, <https://doi.org/10.1016/j.powtec.2016.06.044>.
- [12] M.V. Rodrigues, M.A.S. Barrozo, J.A.S. Gonçalves, J.R. Coury, Effect of particle electrostatic charge on aerosol filtration by a fibrous filter, *Powder Technol.* 313 (2017) 323–331, <https://doi.org/10.1016/j.powtec.2017.03.033>.
- [13] B. Shi, L. Ekberg, Ionizer assisted air filtration for collection of submicron and ultrafine Particles□ evaluation of long-term performance and influencing factors, *Environ. Sci. Technol.* 49 (11) (2015) 6891–6898, <https://doi.org/10.1021/acs.est.5b00974>.
- [14] F.M.O. Silva, M.V. Rodrigues, M.L. Aguiar, O efeito da carga eletrostática na filtração de partículas de cimento em filtros de mangas. *enciclopédia biosfera, Centro Científico Conhecer - Goiânia* 16 (29) (2019) 2420, https://doi.org/10.18677/EnciBio_2019A185.
- [15] A. Wang, Q. Song, G. Tu, H. Wang, Y. Yue, Q. Yao, Influence of flue gas cleaning system on characteristics of PM2.5 emission from coal-fired power plants, *International Journal of Coal Science & Technology* 1 (1) (2014) 4–12, <https://doi.org/10.1007/s40789-014-0001-x>.
- [16] K. Adamiak, A. Krupa, A. Jaworek, Unipolar particle charging in an alternating electric field, Bristol [England], in: *Institute of Physics Conference Series*, vol. 143 Adam Hilger, Ltd., Boston, 1995, pp. 275–278. c1985-.
- [17] Z. Long, Q. Yao, Numerical simulation of the flow and the collection mechanism inside a scale hybrid particulate collector, *Powder Technol.* 215 (2012) 26–37, <https://doi.org/10.1016/j.powtec.2011.08.045>.
- [18] R.P. Donovan, L.S. Hovis, G.H. Ramsey, D.S. Ensor, Electric-field-enhanced fabric filtration of electrically charged flyash, *Aerosol. Sci. Technol.* 1 (4) (1982) 385–399, <https://doi.org/10.1080/02786828208958603>.
- [19] M.D.M. Sepulveda Innocentini, F. Ortega, F. Permeability, m. Sheffler, p. Colombo (Eds.), *Cellular Ceramics: Estructure, Manufacturing, Properties and Applications*, 2005, pp. 313–340.
- [20] C.H. Hung, W.W.F. Leung, Filtration of nano-aerosol using nanofiber filter under low Peclet number and transitional flow regime, *Separ. Purif. Technol.* 79 (1) (2011) 34–42, <https://doi.org/10.1016/j.seppur.2011.03.008>.

- [21] A.C.C. Bortolassi, V.G. Guerra, M.L. Aguiar, Characterization and evaluate the efficiency of different filter media in removing nanoparticles, *Separ. Purif. Technol.* 175 (2017) 79–86, <https://doi.org/10.1016/j.seppur.2016.11.010>.
- [22] M.L. Aguiar, J.R. Coury, Cake formation in fabric filtration of gases, *Ind. Eng. Chem. Res.* 35 (10) (1996) 3673–3679, <https://doi.org/10.1021/ie960042p>.
- [23] R. Kurose, H. Makino, M. Hata, C. Kanaoka, Numerical analysis of a flow passing through a ceramic candle filter on pulse jet cleaning, *Adv. Powder Technol.* 14 (6) (2003) 735–748, <https://doi.org/10.1163/15685520360732016>.
- [24] J.R. Coury, *Electrostatic Effects in Granular Bed Filtration of Gases*, 1983. United Kingdom.
- [25] E.H. Tanabe, P.M. Barros, K.B. Rodrigues, M.L. Aguiar, Experimental investigation of deposition and removal of particles during gas filtration with various fabric filters, *Separ. Purif. Technol.* 80 (2) (2011) 187–195, <https://doi.org/10.1016/j.seppur.2011.04.031>.
- [26] D.C. Walsh, Recent advances in the understanding of fibrous filter behaviour under solid particle load, *Filtrat. Separ.* 33 (6) (1996) 501–506, [https://doi.org/10.1016/S0015-1882\(97\)84316-9](https://doi.org/10.1016/S0015-1882(97)84316-9).
- [27] Bruno José Chiaramonte de Castro, Camila Raquel de Lacerda, Bruna Râmela de Melo, Rafael Sartim, Mônica Lopes Aguiar, Performance assessment of a bench scale hybrid filter in the collection of nanoparticles, *Process Saf. Environ. Protect.* 154 (2021) 32–42, <https://doi.org/10.1016/j.psep.2021.07.042>.
- [28] C.-S. Wang, Electrostatic forces in fibrous filters—a review, *Powder Technol.* 118 (1–2) (2001) 166–170, [https://doi.org/10.1016/S0032-5910\(01\)00307-2](https://doi.org/10.1016/S0032-5910(01)00307-2).
- [29] Q. Huang, H. Shen, Z. Wang, X. Liu, R. Fu, Influences of natural and anthropogenic processes on the nitrogen and phosphorus fluxes of the Yangtze Estuary, China, *Reg. Environ. Change* 6 (3) (2006) 125–131, <https://doi.org/10.1016/j.powtec.2006.01.014>.
- [30] W. Liu, S. Li, A. Baule, H.A. Makse, Adhesive loose packings of small dry particles, *Soft Matter* 11 (32) (2015) 6492–6498, <https://doi.org/10.1039/C5SM01169H>.
- [31] J. Mermelstein, S. Kim, C. Sioutas, Electrostatically enhanced stainless steel filters: effect of filter structure and pore size on particle removal, *Aerosol Sci. Technol.* 36 (1) (2002) 62–75, <https://doi.org/10.1080/027868202753339087>.
- [32] S. Xia, L. Duan, J. Wang, R. Ji, Effect of the surface treatment process of filter bags on the performance of hybrid electrostatic precipitators and bag filters, *Atmosphere* 13 (2022) 1294, <https://doi.org/10.3390/atmos13081294>.